Open access • Journal Article • DOI:10.1021/ACS.MACROMOL.8B01742

Tuning the Thermal Properties and Morphology of Isodimorphic Poly[(butylene succinate)-ran-(ε-caprolactone)] Copolyesters by Changing Composition, Molecular Weight, and Thermal History — Source link

Maryam Safari, Antxon Martínez de Ilarduya, Agurtzane Mugica, Manuela Zubitur ...+3 more authors

Institutions: University of the Basque Country, Polytechnic University of Catalonia, Ikerbasque

Published on: 20 Nov 2018 - Macromolecules (American Chemical Society (ACS))

Topics: Comonomer and Copolyester

Tuning the thermal properties and morphology of isodimorphic poly[(butylene succinate)-ran-(ε-caprolactone)] copolyesters by changing composition, molecular weight and thermal history

Journal:	*Macromolecules*
Manuscript ID	ma-2018-017424.R2
Manuscript Type:	Article
Date Submitted by the Author:	09-Nov-2018
Complete List of Authors:	Safari, Maryam; Universidad del Pais Vasco, Chemistry Martínez de Ilarduya, Antxon; UPC, Chem. Eng Mugica, Agurtzane; Facultad de Químicas (UPV/EHU), ciencia y tecnologia de polimeros Zubitur, Manuela; Escuela Universitaria Politecnica, (UPV/EHU), ingenieria quimica y del medio ambiente Muñoz-Guerra, Sebastián; UPC, Chemical Engineering Müller, Alejandro; Faculty of Chemistry,University of the Basque Country (UPV/EHU), Polymer Science and Technology Department

Tuning the thermal properties and morphology of isodimorphic poly[(butylene succinate)-ran-(ε-caprolactone)] copolyesters by changing composition, molecular weight and thermal history

Maryam Safari[1], Antxon Martínez de Ilarduya[2], Agurtzane Mugica[1], Manuela Zubitur[3], Sebastián Muñoz-Guerra[2], Alejandro J. Müller*[1,4]

[1]*POLYMAT and Polymer Science and Technology Department, Faculty of Chemistry, University of the Basque Country UPV/EHU, Paseo Manuel de Lardizabal, 3, 20018 Donostia-San Sebastián, Spain*

[2]*Departament d'Enginyeria Química, Universitat Politècnica de Catalunya, ETSEIB, Diagonal 647, 08028 Barcelona, Spain*

[3] *Chemical and Environmental Engineering Department, Polytechnic School, University of the Basque Country (UPV/EHU), 2008 Donostia-San Sebastián, Spain*

[4]*IKERBASQUE, Basque Foundation for Science, Bilbao, Spain*

*Corresponding author: alejandrojesus.muller@ehu.es

Abstract

High molecular weight poly[(butylene succinate)-ran-(ε-caprolactone)] copolyesters (PBS-*ran*-PCL) were synthesized in a wide composition range and compared with significantly lower molecular weight samples synthesized previously. DSC and WAXS showed that these copolyesters are isodimorphic (i.e., each crystalline phase contains a small amount of the second comonomer) as they able to crystallize in the entire composition range, display a pseudo-eutectic point, and their unit cell dimensions are a function of composition. Copolymers close or away from the pseudo-eutectic point exhibited a single crystalline phase, i.e., PBS-rich or PCL-rich crystalline phase. At the pseudo-eutectic point, both phases are able to crystallize in double crystalline banded spherulites, as demonstrated by Polarized Light Optical Microscopy (PLOM) studies. An increase in molecular weight of the copolyester does not influence T_m and T_c significantly, as their values are determined by the randomness of the comonomer distribution. However, crystallinity values are higher for lower M_w copolymers because of their faster crystallization rate. Copolymers with higher M_w exhibited higher T_g values as expected for random copolymers that are characterized by a single phase in the amorphous regions. Therefore, changing composition and molecular weight, a remarkable separate control over T_g and T_m values can be achieved in these copolyesters. SAXS results revealed that the lamellar thickness l_c decreases with composition at each side of the eutectic point. Comonomer exclusion limits the length of crystallizable sequences; as a result, the lamellar thickness values do not significantly vary with M_w in the range studied here. At the pseudo-eutectic copolyester compositions, the cooling rate determines for both series of samples (low and high M_w) if one or two crystalline phases can develop: only PCL-rich crystalline phase, only PBS-crystalline phase or both crystalline phases. This behavior was studied in detail by DSC, *in situ* WAXS/SAXS and PLOM. Our studies demonstrate that these biodegradable copolymers are versatile materials, whose properties can be tuned by composition, molecular weight and thermal history to better target specific applications.

Keywords: *Poly(ε-caprolactone), Poly(butylene succinate), random copolyesters, molecular weight, isodimorphism, cooling rate dependence.*

1. Introduction

Crystallizable random copolymers display a wide variety of properties depending on the chemical structure of the two comonomeric units and their composition. Considering two potentially crystallizable components, three different cases are possible, which have been recently reviewed. [1]

The first case is that of total comonomer inclusion inside the crystal unit cell, or co-crystallization in the entire composition range. A plot of melting temperature versus composition yields a straight line that follows a simple rule of mixtures. These copolymers are denoted as isomorphic. [2, 3] In the case of copolyesters, very few cases of isomorphism have been reported, [4-7] and they occur when the chemical structure of both comonomers are very similar.

The second case occurs when the chemical structure of the two constituent comonomers differ more than in the previous case. A competition between exclusion and inclusion (inside the crystal lattice) of the minor comonomer component with respect to the major comonomer component is established during crystallization. But in these copolymers, there is always a small amount of inclusion of the second comonomer within the crystal unit cell of the majority comonomer. As a result, the copolymers crystallize in the entire composition range and are classified as isodimorphic. This means that two crystalline phases are formed with crystal structures that resemble those of the parent homopolymers. When the melting temperature is plotted as a function of composition, a pseudo-eutectic point is observed. To each side of the eutectic, only one crystalline phase is formed, that is rich in the major component with limited inclusion of the second comonomer. We have recently found that at the eutectic point, two crystalline phases can co-exist depending on the thermal history, with crystalline unit cells

resembling those of the parent homopolymers.[1] Several isodimorphic random copolyesters have been recently studied. [8-18]

The third and final case is that of total exclusion of the minor comonomeric units and it is the most frequently reported case, when the chemical structures of the comonomers are very different from one another. For random copolyesters, this behavior has been reported by Soccio et al. in poly(propylene isophthalate-*ran*-propylene succinate)[19] and poly(propylene isophthalate-*ran*-propylene adipate). [20]

Aliphatic biodegradable polyesters, such as poly (butylene succinate) (PBS) and poly (ε-caprolactone) (PCL) have received much attention since they are potentially biodegradable and may contribute to reduce environmental pollution caused by plastic waste. [21, 22] The combination of PCL and PBS as random or block copolyesters, has been used to design new materials with improved behavior and performance. [23, 24] The mechanical and functional properties of semicrystalline polymers depend on structural and morphological features that are controlled by their molecular weight and crystallization conditions during processing. [25, 26] To enhance product performance of random copolyesters for specific applications, it is essential to know in detail how the molecular weight and composition influence their main properties.

Recently, we synthesized poly[(butylene succinate)-ran-(ε-caprolactone)] s (PBS-ran-PCL) by enzymatic ring opening polymerization. The copolyesters obtained had low molecular weights (in most cases the weight average molecular weight was lower than 6000 g/mol), but they displayed a remarkable isodimorphic behavior. [27] In this work, higher molecular weight poly (butylene succinate-*ran*-caprolactone)s (PBS-*ran*-PCL) copolyesters were prepared in a wide composition range by changing the synthetic strategy to a direct transesterification/ROP and polycondensation route. A detailed comparison between the results obtained with the

presently synthesized high molecular weight copolyesters (denoted HM_w BS_xCL_y, where x and y are the molar % of BS and CL units respectively) and our previous series of copolyesters with lower molecular weight (denoted LM_w BS_xCL_y) [27] is presented.

Cao *et al.* [28] also prepared PBS-*ran*-PCL copolymers with a similar synthetic approach. However, to the best of our knowledge, this is the first time that the non-isothermal crystallization and thermal transitions of these copolymers have been studied as a function of molecular weight. In the current investigation, non-isothermal crystallization of HM_w BS_xCL_y and their parent homopolymers are studied by means of polarized light optical microscopy (PLOM), differential scanning calorimetry (DSC), *in situ* simultaneous synchrotron wide angle X-ray scattering (WAXS) and small angle X-ray scattering (SAXS). We investigate the role of molecular weight and composition on the thermal properties, structure and crystallization of these random copolyesters. Additionally, we have found remarkable results at the pseudo-eutectic composition by varying the cooling rate from the melt, so that the formation of one or two crystalline phases can be controlled.

2. Experimental

Materials

Dimethyl succinate (DMS), 1,4-butanediol (BD), titanium tetraisopropoxide (TTP) catalyst, and ε-caprolactone (CL) were purchased from Aldrich company. All materials were used as received.

Synthesis of HM_w BS_xCL_y

Concisely, for the $BS_{51}CL_{49}$ a three-necked 50 ml flask was charged with 1.46 g (10 mmol) of dimethyl succinate (DMS), 1.38 g (15 mmol) of 1,4-butanediol (BD), and 1.140g (10 mmol) of ε-caprolactone. DMS /CL mixtures at molar ratios of 90/10, 80/20,70/30, 60/40, 55/45, 50/50, 45/55, 40/60, 30/70, 20/80 and 10/90, were used so the whole range of compositions was essentially covered.

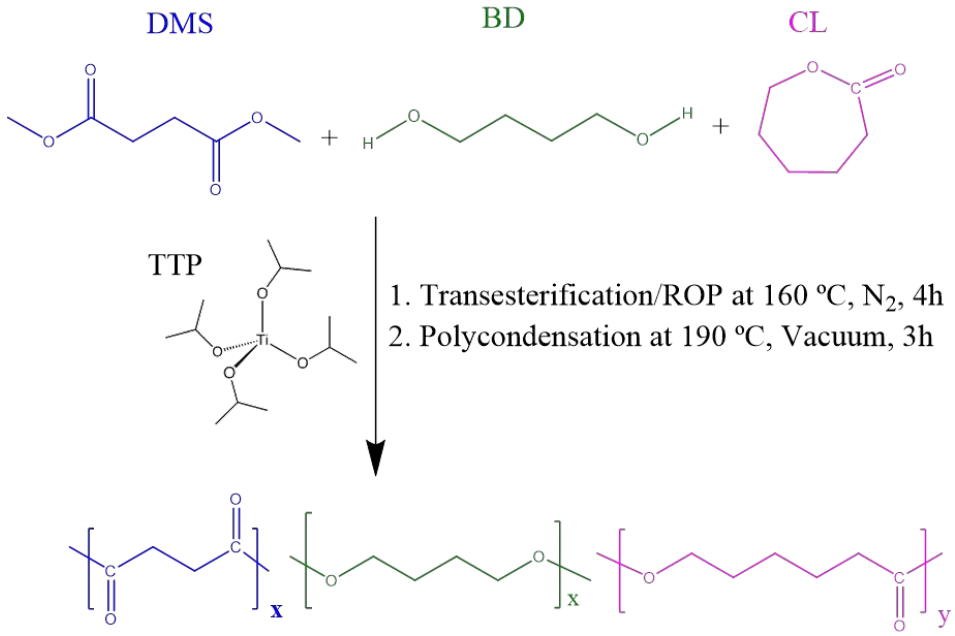

Scheme 1. Synthetic route for the preparation of HM_w BS_xCL_y.

The mixture was left under mechanical stirring in a thermostatized silicon oil bath until the temperature stabilized at 160 °C and the medium became homogeneous. Then 0.16 µl (0.0005 mmol) of TTP with the TTP/ε-CL molar ratio equal to 0.005 % were added under gentle agitation at 50 rpm. The transesterification/ROP reaction was conducted for 4h and finally the polycondensation was performed under gradually reduced pressure to a final value of 0.1 mm

Hg at 190 ºC for around 3 h. The high molecular weight values are possibly due to the high vacuum applied during the polycondensation step. The same process was carried out for the synthesis of the corresponding homopolyesters PBS and PCL using DMS and ε-CL as respective feeds. Scheme 1 shows the route leading to HM_w BS_xCL_y copolyesters using TTP catalyst.

Table 1. Synthesis results of the copolymerization of butylene succinate and ε-caprolactone.

Polyester	Composition[a] (BS/CL mol/mol)		Molecular weight[b] (g/mol)			Microstructure[c] (S-centered triads content)			
	Feed	Found	M_n	M_w	$Đ$	BSB	BSCL/CLSB	CLSCL	R
PBS	100/0	100/0	7500	21470	2.9	-	-	-	-
$BS_{91}CL_9$	90/10	91/09	8790	21640	2.5	1	21	78	1.08
$BS_{78}CL_{22}$	80/20	78/22	6580	18000	2.7	4	23	73	1.03
$BS_{66}CL_{34}$	70/30	66/34	7830	19700	2.5	9	37	54	1.05
$BS_{62}CL_{38}$	60/40	62/38	9750	27300	2.8	9	38	53	1.05
$BS_{55}CL_{45}$	55/45	55/45	8970	24700	2.7	10	39	51	0.98
$BS_{51}CL_{49}$	50/50	51/49	7400	23500	3.1	17	45	41	1.00
$BS_{45}CL_{55}$	45/55	45/55	8000	17300	2.2	20	43	37	1.03
$BS_{38}CL_{62}$	40/60	38/62	11000	24300	2.2	25	47	28	1.05
$BS_{34}CL_{66}$	30/70	34/66	10000	29900	2.2	27	50	23	1.08
$BS_{27}CL_{73}$	20/80	27/73	11540	28700	2.5	31	48	21	1.05
$BS_{11}CL_{89}$	10/90	11/89	6300	19500	3.1	55	40	5	0.98
PCL	0/100	0/100	5400	17400	3.2	-	-	-	-

[a] Composition of the feed and the resulting polymer as determined by ^{1}H NMR.
[b] Number and weight average molecular weights and dispersities estimated by GPC against PMMA standards.
[c] Copolyester microstructure determined by NMR; *R* is the degree of randomness which should be 1 for a fully statistical distribution of the comonomeric units.

Table 1 shows molecular weight and microstructural data for the synthesized copolyesters in the presence of TTP catalyst. The microstructure of the prepared copolyesters is essentially random as judged by the triads contents and R values given in Table 1. NMR results confirm the chemical structure of copolyesters. ^{1}H and ^{13}C NMR spectra, of the $BS_{51}CL_{49}$ copolyester are shown in Figure SI-1 (see Supporting Information), and the spectra of the entire series are compared in Figure SI-2.

The weight average molecular weights (M_w) of the HM_w BS_xCL_y copolyesters are in the range 17000- 30000 g/mol with dispersities ($Đ$) between 2.2 and 3.2. Overall, the M_w of HM_w BS_xCL_y copolyesters are approximately four times higher than most of the similar copolyesters previously synthesized by enzymatic (CALB) ROP copolymerization (LM_w BS_xCL_y) in our previous work (see Table SI-1). [27]

Nuclear Magnetic Resonance (NMR)

The ^{1}H NMR and ^{13}C NMR spectra were operated at 300.1 and 75.5 MHz respectively, on a Bruker AMX-300 NMR instrument. The samples were dissolved in deuterated chloroform and TMS was used as internal reference. Quantitative ^{13}C NMR spectra were recorded applying an inverse gated decoupling pulse sequence to avoid nuclear Overhauser effect (NOE) enhancement of the ^{13}C NMR signals, and using long delay times. The composition of ε-caprolactone repeating unit present in BS_xCL_y was estimated from methylene proton resonance integrals of CH_2 (1) and CH_2 (4). Moreover, the sequence distributions of BS and CL repeating units were calculated based on ^{13}C NMR signals of the methylene group CH_2 (b) in Figure SI-1.

Gel Permeation Chromatography (GPC)

Molecular weight properties were measured by Gel Permeation Chromatograms (GPC) that were acquired at 35 °C with a Waters equipment, a refraction index detector and poly (methyl methacrylate) (PMMA) standards. The samples were chromatographed with 0.05 M sodium trifluoroacetate-hexafluoroisopropanol (NaTFA-HFIP) using a poly(styrene-*co*-divinyl benzene) packed linear column at a flow rate of 0.5 ml/min.

Thermal behavior

Differential Scanning Calorimetry (DSC) experiments were performed using a Perkin Elmer 8500 calorimeter equipped with a refrigerated cooling system Intracooler 2P, under a nitrogen atmosphere flow of 20 ml/min and calibrated with high purity indium and tin standards. Samples crystallization experiments were hermetically sealed in standard aluminum pans and tested according to the following protocol: Samples were heated from room temperature to 30 °C above their melting temperature (T_m) and held at this temperature for 3 min to erase thermal history. They were then cooled to -60°C and reheated again to 30 ºC above their T_m. Measurements were done at two different scan rates, 20 °C/min and 10 °C/min, with the purpose of evaluating the scan rate effect on melting and crystallization behavior. The melting temperature T_m was determined from the second scan as the temperature of the main peak in the DSC curves.

To determine the glass transition temperature (T_g), samples were heated from room temperature to 140 °C (for BS-rich samples) or 90 °C (for CL-rich samples) at a rate of 10 °C/min. They were then cooled using the ballistic cooling option of DSC 8500, which cools the sample at an average nominal rate of approximately 160 ºC/min) to -90 °C. Finally, the sample was heated to 140 °C (for BS-rich samples) or 90 °C (for CL-rich samples) at a rate of 20

°C/min. The glass transition temperatures, T_g, were calculated from the DCS scans as the midpoint of the heat capacity change.

X-ray diffraction

The samples were examined under non-isothermal conditions by simultaneous *in situ* WAXS/SAXS performed at beamline BL11-NCD at the ALBA Synchrotron radiation facility, in Barcelona, Spain. The samples in DSC pans were placed in a Linkam THMS600 stage coupled to a liquid nitrogen cooling system. Firstly, they were heated at 10 °C/min from room temperature to 30 °C above the melting temperature T_m and held for 3 min to erase their thermal history. Secondly, the samples were cooled down to -60 ºC at a rate of 10 ºC/min and held at this temperature for 5 min. Thirdly, the samples were heated up to 30 ºC above the melting point at 10 ºC/min rate. During the mentioned protocol, SAXS/WAXS spectra were recorded every 10 seconds.

WAXS and SAXS scans were taken periodically at two scans per degree centigrade. The energy of the X-ray source was 12.4 keV (λ = 1.0 Å). In the WAXS configuration, the sample-detector (WAXS detector, Rayonix LX255-HS with an active area of 230.4×76.8 mm (pixel size: 44 μm^2)) distance employed was 15.5 mm with a tilt angle of 27.3°. In the case of the SAXS configuration, the sample-detector (SAXS detector, Pilatus 1M (from Dectris)) had an activated image area of 168.7×179.4 mm^2, a total number of pixels of 981×1043, 172×172 μm^2 pixels size , frame rate of 25 frames/sec, and the distance employed was 6463 mm. The intensity profile was output as the plot of the scattering intensity vs scattering vector, q=4πsinθλ^{-1}, where λ is the X-ray wavelength (λ = 1 Å) and 2θ is the scattering angle. The scattering vector was calibrated using silver behenate (SAXS) and chromium (III) oxide (WAXS).

Polarized Light Optical Microscopy (PLOM)

A polarized light optical microscope, Olympus BX51 equipped with an Olympus SC50 digital camera and in combination with a Linkam TP-91 hot stage was used to observe spherulite development. Films with around 10 μm thickness were prepared by melting the samples in between two glass slides. For non-isothermal experiments, the samples were first heated to 30 °C above their melting point T_m to erase their thermal history and then they were crystallized from the melt by cooling to 20 ºC below their crystallization temperature T_c at 10 °C/min.

Results and Discussion

The thermal behavior of the samples was explored by non-isothermal DSC experiments. The samples were first heated to a temperature high enough to erase their thermal history, and then they were cooled at 10 ºC/min. After this controlled cooling, their melting behavior was recorded in the DSC second heating scans shown in Figure 1a. The previous cooling runs as well as the calorimetric data derived from all the DSC non-isothermal runs can be found in the Supplementary Information (see Figure SI-3 and Tables SI-2 and SI-3).

Figure 1a shows that these random copolymers are able to crystallize in the entire composition range, even for compositions close to equimolarity. As demonstrated by NMR, the copolymers are random (see Table 1, values of R=1 indicate complete randomness). Only isomorphic or isodimorphic random copolymers can crystallize in the entire composition range. However, Figure 1b illustrates that the melting point follows a pseudo-eutectic trend with composition indicating that the HM_w PBS-*ran*-PCL copolymers are isodimorphic.[1, 3] In the HM_w $BS_{45}CL_{55}$ sample, there are two melting temperatures and two crystallization temperatures

indicating the presence of two crystalline phases at the eutectic point, i.e., a PCL-rich and a PBS-rich crystalline phases.

Figure 1b also illustrates the tremendous versatility of these random copolyesters. Thanks to their isodimorphic character, their melting point can be tailored by changing composition with a variation of 100 ºC.

In isodimorphic copolymers, the comonomer that constitutes the major phase typically crystallizes with the unit cell of its corresponding homopolymer, but including a small number of comonomer units of the minor second component within the crystal lattice. There is always a competition between comonomer exclusion and comonomer inclusion in isodimorphic copolymers. Their behavior is typically dominated by a higher amount of comonomer exclusion but comonomer inclusion is indispensable for crystallization in the entire composition range.

According to WAXS results (see Figure 1c), to the left side of the pseudo-eutectic point, only PBS-like crystals are formed and to the right side of this point, only PCL-like crystals are found. The indexation of the WAXS patterns can be found in the Supporting Information along with WAXS data taken at different temperatures (see Figures SI-7 and Table SI-4 and Table SI-5). In HM_w BS_xCL_y copolymers, for the composition that corresponds to the eutectic point ($BS_{45}CL_{55}$), two crystalline phases (PBS-rich crystalline phase and PCL-rich crystalline phase) were found that correspond to those observed by DSC (See figure SI-3 and table SI-2).

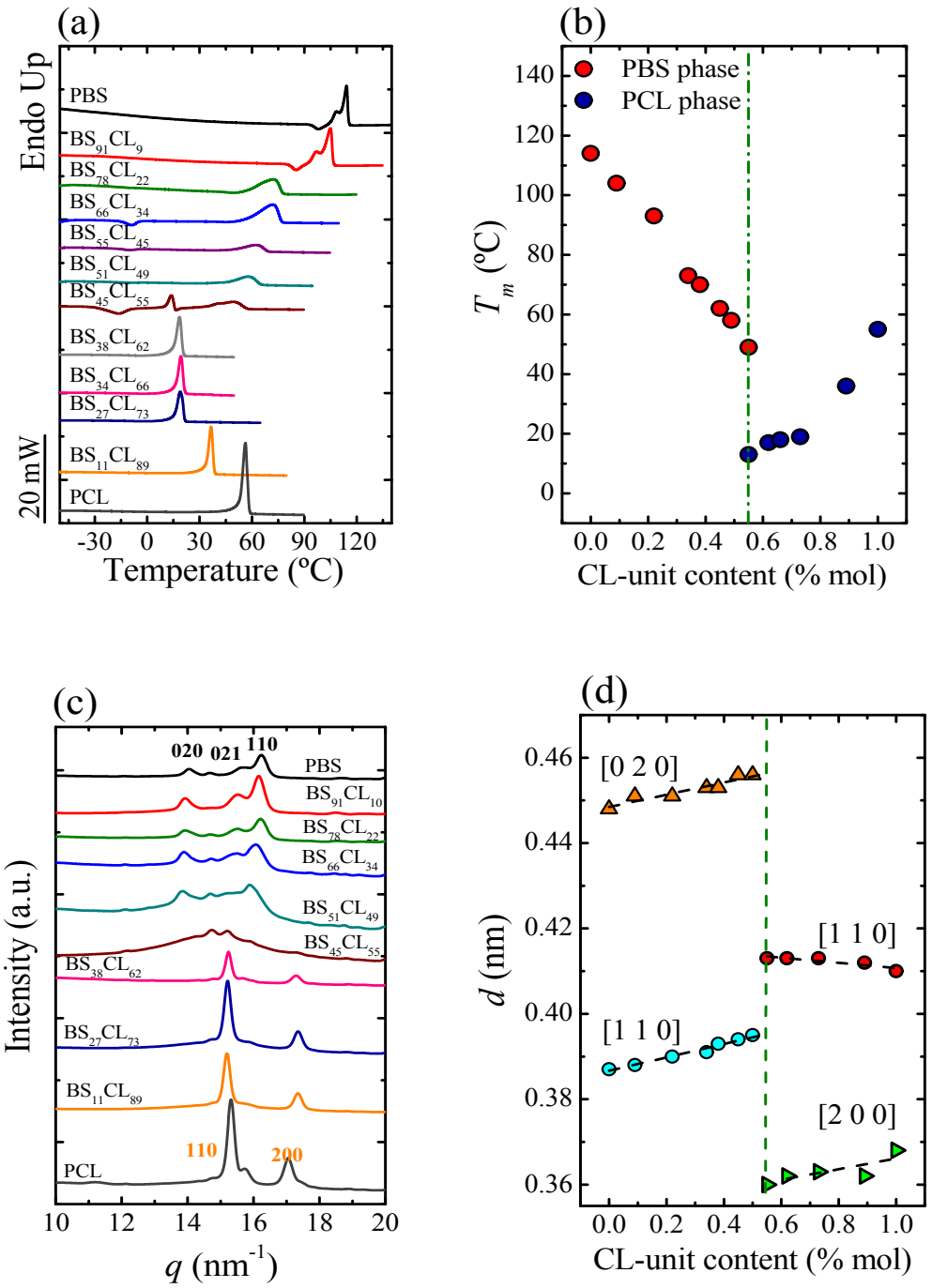

Figure 1. (a) DSC second heating runs at 10 ºC/min for the indicated HM_w samples. (b) Peak melting temperature as a function of composition, the dashed vertical line indicates the pseudo-eutectic composition. (c) WAXS diffraction patterns taken at -60 ºC after cooling from the melt at 10 ºC/min. (d) *d*-spacings obtained from the WAXS results presented in (c) as a function of composition.

The *d*-spacings observed in the WAXS profiles registered at -60 ºC versus CL unit content are plotted in Figure 1d. At -60 ºC, *d*-spacings for PBS-rich crystalline phases arising from (020) and (110) planes, as well as those for PCL-rich crystalline phases corresponding to (110) planes, display an increasing trend with comonomer content. These increases correspond to changes in unit cell sizes that reflect a certain degree of comonomer inclusion that takes place within the crystal unit cells of the corresponding crystal phases of these random copolymers. The *d*-spacings observed in the WAXS profiles registered versus CL-unit content at -60 ºC and 25 ºC are compared in Figure SI-8.

The results presented in Figure 1 are fully consistent with the isodimorphic character of the HM_w PBS-*ran*-PCL copolymers. These results are qualitatively similar to those obtained previously by us with LM_w PCL-*ran*-PBS copolymers.[27] The specific differences observed between low and high M_w copolymers are discussed in the next section.

We studied the effect of copolymer composition on the spherulitic texture of HM_w PCL-*ran*-PBS copolyesters. Figure SI-5 shows PLOM micrographs during non-isothermal crystallization, after spherulites had impinged on each other for HM_w copolymers. The incorporation of comonomer units has a strong impact on nucleation of the majority phase spherulites. Increasing the amount of comonomer unit content leads to the formation of a higher concentration of spherulites with smaller sizes, indicating an increase in nucleation density. These results are very similar to those obtained previously with LM_w BS_xCL_y.[27] In both cases, adding comonomer enhances nucleation density during non-isothermal crystallization, thereby decreasing spherulitic size.

HM_w $BS_{45}CL_{55}$ is a random copolymer whose composition corresponds to the pseudo-eutectic point. This is the only copolymer from those HM_w random copolyesters prepared in

this work that exhibited a double crystalline morphology. We have previously found that only those copolymers at the pseudo-eutectic point or pseudo-eutectic region are able to exhibit double crystallization. [1, 16, 27, 29]

Figure 2a shows PBS-rich spherulites after the HM_w $BS_{45}CL_{55}$ sample was cooled from the melt and held at 20 ºC for 2 h. At this temperature, the PCL-rich crystals are in the melt (see Figure 1a and 1b), and negative ring banded PBS-rich spherulites fill the microscope field. Therefore, upon cooling from a single phase melt, the PBS-rich phase is the first to crystallize forming spherulitic templates. These impinging spherulites contain lamellar crystals of the PBS-rich phase with amorphous interlamellar regions of copolymer chains. A schematic diagram representing these spherulites is also included in Figure 2a, only the crystalline PBS-rich lamellae growing radially are represented.

Figure 2b shows the result of quenching the sample shown in Figure 2a from 20 ºC down to -25 ºC, a temperature at which the PCL-rich phase can crystallize within the intraspherulitic region of the PBS-rich phase (i.e., within the interlamellar regions of the spherulite). The crystallization of the PCL component can be observed in Figure 2b, as the birefringence increases in the sample and the spherulitic structures look brighter (compare the close up spherulite shown in Figure 2a, before PCL crystallization with that in Figure 2b, after PCL-rich crystals are formed).

The PBS-rich phase crystals templates the crystalline superstructural morphology (blue lamellae in schematic model of Figure 2a), and the PCL-rich crystals can only form upon cooling from the melt (see red inner lamellae in Figure 2b) inside the pre-formed templates. Hence, in Figure 2b we have examples of double crystalline spherulites.

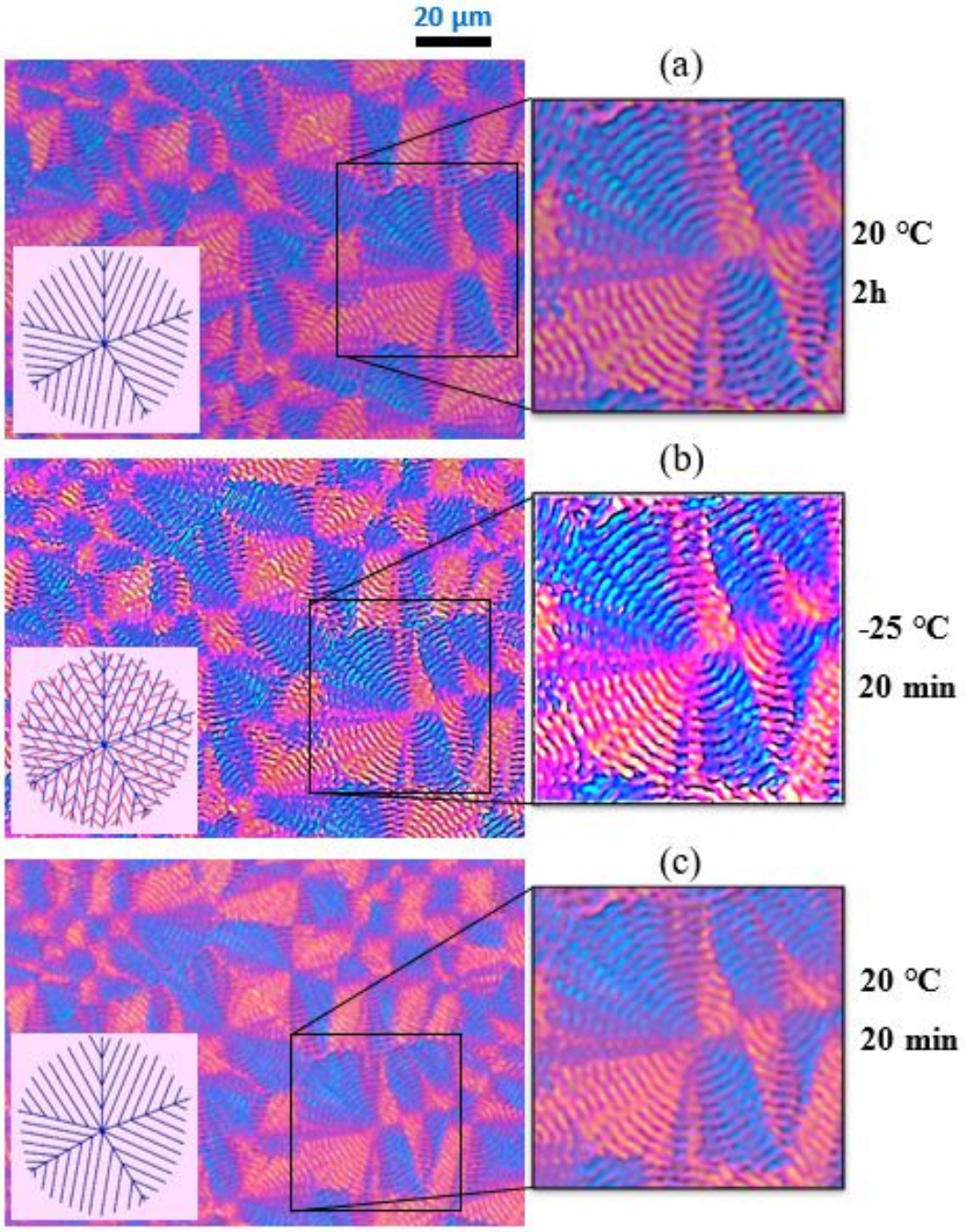

Figure 2. PLOM micrographs for HM_w $BS_{45}CL_{55}$ copolymer with schematic models: (a) the sample was cooled from the melt and held at 20 ºC for 2h, (b) micrograph taken after the sample was quenched rapidly from 20 ºC to -25 ºC and held 20 min at -25 ºC, and (c) sample was reheated to 20 ºC. In the schematic models (bottom left hand side), the blue lines indicate PBS-rich lamellae while the red lines correspond to PCL-rich lamellae and the pink background indicates the amorphous regions of homogeneous mixtures of copolymer chains.

Similar double crystalline superstructures have been observed in PBS-*ran*-PBAz copolyester at the pseudo-eutectic composition [29] and in weakly segregated or melt mixed block copolymers. [30, 31]

Figure 2c shows the morphology after the sample was reheated up to 20 °C to melt the PCL-rich phase crystals. The field remains full with PBS-rich phase spherulites as expected since the molten PCL-rich phase is within the intraspherulitic regions of the PBS phase.

Influence of molecular weight on crystallization and melting

In this work, only one of the prepared compositions fell within the eutectic point (i.e., HM_w $BS_{45}CL_{55}$), as signaled by the presence of two crystalline phases.[1] When the composition was changed to $BS_{38}CL_{62}$ (i.e., 7 molar % more CL units in the copolymer with respect to the eutectic composition), then only the PCL-rich crystalline phase was formed. On the other hand, when it was changed to $BS_{51}CL_{49}$ (i.e., 6 molar % less CL units than the eutectic composition) just the PBS-rich crystalline phase was formed, see Figure 1.

In the LM_w BS_xCL_y case, three copolymers were inside the eutectic region ($BS_{45}CL_{55}$, $BS_{48}CL_{52}$, and $BS_{54}CL_{46}$) as for these copolyesters two characteristic crystallization and melting peaks were observed.[27] These three copolyesters span a CL composition range of 11 molar %. Therefore, lower molecular weights apparently cause a widening of the pseudo-eutectic region in these isodimorphic systems. However, more compositions would have to be prepared to confirm this trend.

A comparison between the non-isothermal crystallization and melting of both sets of samples can be observed in Figure 3. As it is well known, in homopolymers, T_m values increase with chain length until they saturate at high molecular weights. Figure 3 clearly shows that in

these random copolyesters, both T_c and T_m are not affected by the changes in molecular weight. This result can be explained as in random copolymers, the comonomeric content and its distribution can dominate the crystallizable sequence selection during crystallization. [12, 32] As both types of copolymers are nearly perfectly random, the size of the average crystallizable sequence is clearly much lower than the lowest M_w copolymer chain length.

Figures 3c and 3d show how the enthalpy of crystallization and melting (normalized by the content of the crystallizable phase) depend on copolymer composition. Figure 3e plots the degree of crystallinity (obtained from the DSC heating scans) as a function of composition. Two important observations can be made from these plots.

Firstly, the degree of crystallinity displays a pseudo-eutectic point when plotted as a function of composition. This is a consequence of the influence of comonomer exclusion during crystallization. As the amount of comonomer increases for a particular crystalline phase (either PBS-rich or PCL-rich crystalline phases), comonomer exclusion (which predominates over comonomer inclusion) interferes with crystallization, as the length of crystallizable sequences (which can include a limited number of the second comonomer units) decreases. As a consequence, the degree of crystallinity decreases when the minority comonomer content increases for any given crystalline phase.

Secondly, Figures 3c-3e show that the lower molecular weight samples can develop a higher degree of crystallinity than the higher molecular weight copolymers. This is due to their higher non-isothermal crystallization rate, which stems from the faster diffusion of smaller molecules.

The crystallinity of copolyesters has been determined by dividing the observed heat of fusion ΔH_m by the theoretical value for 100% crystalline polymer. The theoretical ΔH_m^0 values for PBS and PCL are 110.3 and 139.5 J/g, [33, 34] respectively. The data for the copolymers plotted

in Figure 3e show that the crystallinity levels are sensitive to molecular weight, as well as, to the copolymer composition.

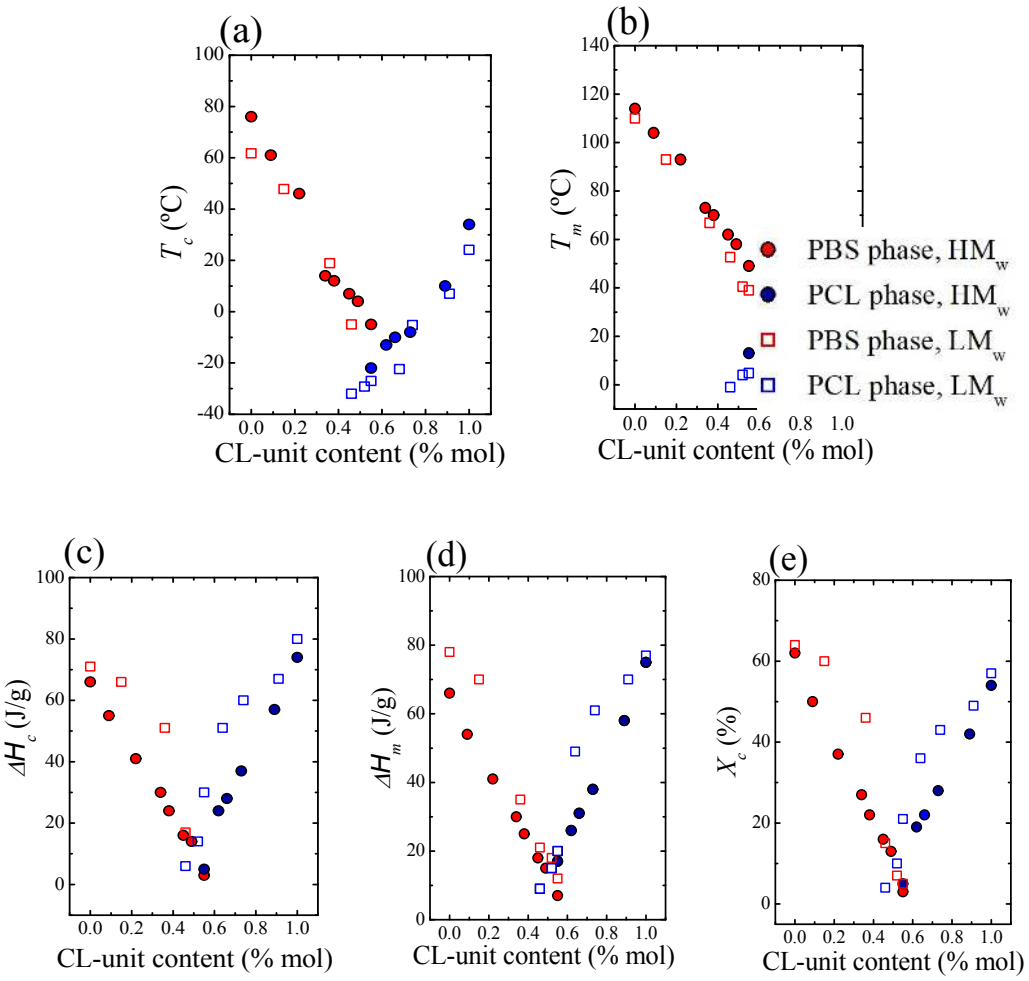

Figure 3. Composition dependence of (a) peak crystallization temperature T_c (b), peak melting temperature T_m, (c) crystallization enthalpy ΔH_c, (d) melting enthalpy ΔH_m, and (e) crystallization degree X_c of the indicated samples.

Influence of molecular weight on T_g

Random copolymers form a single phase in the melt and in the amorphous state. They exhibit a single T_g that depends on composition. Figure 4 shows how the T_g, in both copolymer groups (low and high molecular weight), is a strong function of composition and molecular weight. For both homopolymers and random copolymers, T_g values increase with molecular weight until they saturate at a limiting molecular weight value. This trend is explained by the higher fraction of chain ends present in lower M_w polymers that can increase the free volume. As the M_w increases the effect of chain ends is diluted and it becomes negligible for very long chains. [35]

In random copolyesters, T_g is usually a monotonic function of composition that can be predicted by semi-empirical equations. In this work, the Gordon-Taylor equation[36] (i.e., Equation 1), was found to adequately describe the experimental data for both types of samples (LM_w and HM_w)

$$T_{g,copo} = \frac{w_1 T_{g,1} + k(1 - w_1) T_{g,2}}{w_1 + k(1 - w_1)} \qquad \text{Eq.1}$$

where $T_{g,1}$ and $T_{g,2}$ are the glass transition temperature of the homopolyesters, w_1 the respective mass fraction of one of the components and k the Gordon-Taylor parameter.

PBS and PCL homopolymers were used for comparison purposes only. In the case of PCL, the values of M_w do not differ much (16.3 and 17.4 kg/mol) but their dispersities are quite different (2 and 3.2 for the low and high M_w samples respectively). This may explain the differences in T_g observed in Figure 4, as the PCL sample with a lower dispersity probably contains a higher density of chain ends.

In the case of PBS homopolymer, even though the differences in M_w between the samples are larger than in the case of PCLs, the observed difference in T_g is very small. We do

not have an explanation for this result. It should be considered that as the crystallinity increases (the homopolymers have crystallinity degrees around 50%), determination of T_g values by DSC become increasingly difficult, especially if a rigid amorphous phase develops in the material. Further studies would be needed that are outside the scope of the present investigation.

As shown in Figure 4, the Gordon-Taylor equation fits well the experimental data with $k = 0.62$ for HM_w samples and $k = 0.23$ for LM_w samples. The term k in Equation 1 is a parameter whose value depends on the change in thermal expansion coefficient (α) of the components as they change from the glassy (amorphous) to the liquid (rubbery) form, during the glass transition. Accordingly, $k = (V_2/V_1)(\Delta\alpha_2/\Delta\alpha_1)$[36], where V represents the specific volume at the corresponding T_g. By the Simha-Boyer law [37] ($\Delta\alpha.T_g$ = constant) we obtain $k \approx (V_2T_{g1}/V_1T_{g2})$ [38]. As far as we are aware, density values for the PBS and PCL homopolymers at the glass transition temperatures are not available. Further studies would be needed to understand in detail the differences in k values beyond a simple fit parameter [39], however, they are beyond the scope of the present study.

If a comparison is made between Figure 3b and Figure 4, a very interesting characteristic of isodimorphic random copolymers can be appreciated. These copolymers allow a separate control of T_m and T_g, both as a function of composition and molecular weight. While in homopolymers both T_m and T_g follow similar empirical correlations as molecular weight increases, in isodimorphic copolymers T_g is a function of M_w while T_m is independent of M_w, as long as the average length of the crystallizable sequences is smaller than the molecular weights of the random copolymers under consideration.

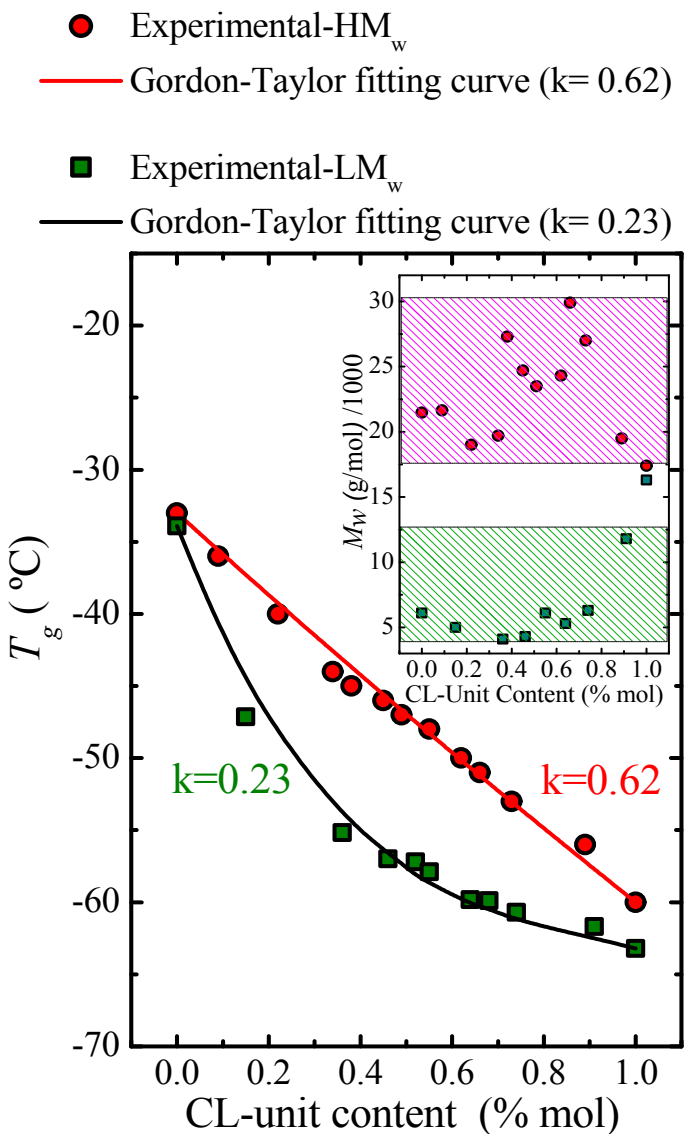

Figure 4. Glass transition temperature as a function of composition for the indicated samples. The inset plots show the M_w values of the samples.

Influence of composition on lamellar thickness

Figures 5a-5d show SAXS diffractograms for all HM_w and LM_w PBS-*ran*-PCL copolymers and parent homopolymers measured at -60 ºC, after the samples were cooled from the melt at 10 ºC/min. In all cases, a single scattering peak can be observed. This reflection

arises from the X-ray scattering produced by lamellar stacks within the spherulitic structures in the sample. From the position of this peak, the long period (L) can be calculated.

In two samples (LM_w $BS_{45}CL_{55}$ and HM_w $BS_{45}CL_{55}$), no SAXS signal was detected, as these samples crystallize a very small amount (approximately 10% or less) during cooling at 10 ºC/min and there was probably not enough lamellar stacking or the long period was so large (as the sample is 90% amorphous) that it fell at angles that are too low for detection.

Figure 5e shows a plot of the lamellar stacks long period determined at -60 ºC as a function of composition for HM_w and LM_w copolyesters. For both HM_w and LM_w BS-*ran*-CL, there is an increase in long period in the PBS rich phase, as the amount of CL units increase in the copolymer. On the right hand side of the pseudo-eutectic point the trend in the data is not so clear in terms of long period values (as they depend on crystallinity, see below).

Another important result is that the long period (Figure 5e), which is inversely proportional to crystallinity, is higher for the HM_w samples in the PBS rich phase, as they contain a higher amount of interlamellar amorphous regions (i.e., the X_c values are lower for HMw copolymers as shown in Figure 3e). While Figure 3b showed how T_m values exhibited almost no difference between low and high M_w samples (for HM_w samples T_m values are slightly higher than for LM_w copolymers), the crystallinity in HM_w copolymers (Figure 3e) was substantially lower than for low M_w copolymers.

The average crystalline lamellar thickness, l_c, of LM_w and HM_w PS-*ran*-PCL samples at -60 ºC were calculated by the approximation: $l_c = L.X_c$ (where X_c is the crystallinity degree and L the long period) and plotted as a function of CL-content in Figure 5f. It can be observed that the lamellar thickness values, within the experimental errors of the measurements, are quite similar between low and high M_w samples (the lamellar thickness are slightly higher, only about

1 nm difference, for HM_w copolymers in consistency with the T_m values trend plotted in Figure 3b).

The l_c values for PBS-rich and PCL-rich copolymers decrease with increases of comonomer unit content and in contrast, the intervening amorphous layer thickness, l_a, values ($l_a = L\text{-}l_c$) increase with comonomer content. These trends in l_a and l_c are fully consistent with the changes of T_m and X_c values as a function of composition presented in Figure 3. In fact, for both series of copolymers, l_a and l_c values also exhibit a pseudo-eutectic-like behavior as a function of composition. The results can be explained if we consider that as comonomer content increases in each phase (i.e., PCL rich crystalline phase or PBS rich crystalline phase) exclusion of the second comonomer predominates. Comonomer exclusion limits the average length of the crystallizable sequences and therefore the lamellar thickness (l_c) decreases. Comonomer exclusion also limits the amount of crystals that can be formed and the degree of crystallinity decreases with CL units content while L and l_a increase.

Moreover, Figure 5f shows that the molecular weight (in the range explored here) does not affect the lamellar thickness values (l_c). These results support our conclusion that in these isodimorphic random copolymers, the random sequence of linear crystallizable chains controls the length of the crystallizable sequences (which is always smaller than the average chain length of LM_w copolymer chains), and therefore the thickness of the lamellae formed. As a consequence, T_m values do not significantly change (as they are directly proportional to the lamellar thickness values, as predicted by the Gibbs-Thompson equation), when the molecular weight of these random copolyesters is increased from the low M_w to the high M_w copolymer series.

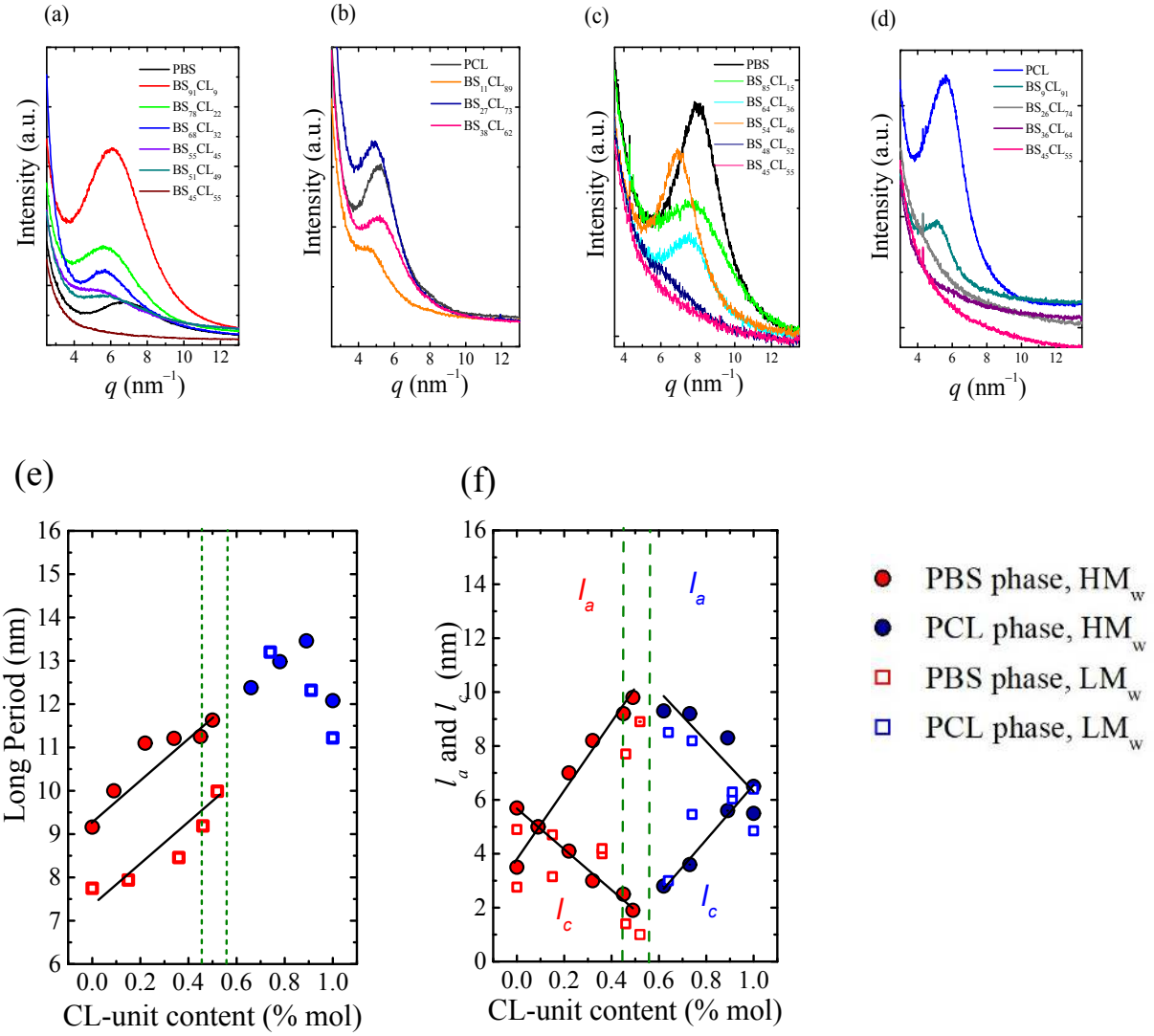

Figure 5. SAXS diffractograms for (a) HM_w-PBS-rich phases, (b) HM_w-PCL-rich phases, (c) LM_w-PBS-rich phases and (d) LM_w-PCL-rich phases at -60 ºC. (e) Long period values as a function of composition for HM_w and LM_w BS-*ran*-CL. (f) Average lamellar thickness (l_c) and amorphous layer thickness (l_a) for HM_w and LM_w BS-*ran*-CL. Solid lines are drawn to guide the eye.

Influence of the cooling rate on non-isothermal crystallization for compositions close and at the pseudo-eutectic point

In order to better understand the sequential and coincident crystallization processes at and near the pseudo-eutectic point, rate-dependent experiments were performed. Figure 6a, 6b, and 6c show cooling scans from the melt at different cooling rates corresponding to the following HM_w copolymers: $BS_{51}CL_{49}$, $BS_{45}CL_{55}$ and $BS_{38}CL_{62}$, respectively. These compositions are located left of the pseudo-eutectic point, at the pseudo-eutectic point, and right of the pseudo-eutectic point. Subsequent heating scans performed at the constant rate of 20 °C/min are shown in Figures 6d, 6e, 6f. Similar experiments were performed with the LM_w samples, and they are presented in the Supplementary Information (Figure SI-6) and commented below when relevant.

At the pseudo-eutectic point of HM_w copolyesters, Figure 6b shows that when the $BS_{45}CL_{55}$ copolymer is cooled at a very slow rate (0.5 and 1 °C/min), only the PBS-rich phase can crystallize, as indicated by the subsequent DSC scan (see Figure 6e), where a single melting peak (with some bimodal character) at temperatures higher than the melting point of the PCL-rich phase can be observed. In this sample, when the PBS-rich phase has enough time to crystallize during cooling, it inhibits the crystallization of the PCL-rich phase at lower temperatures. This is probably due to confinement effects, as the PBS-rich phase crystallizes from the melt into well-develop spherulitic superstructures (of small size according to PLOM observations, see Figure SI-5) formed by radially growing PBS-rich lamellae. Upon further cooling, the PCL-rich lamellae would have to crystallize in the interlamellar regions of these PBS-rich spherulitic templates. Similar results were obtained for poly[(butylene succinate)-*ran*-

(butylene adipate)] [16] and poly[(butylene succinate)-*ran*-azelate] copolymers at the pseudo-eutectic point. [40]

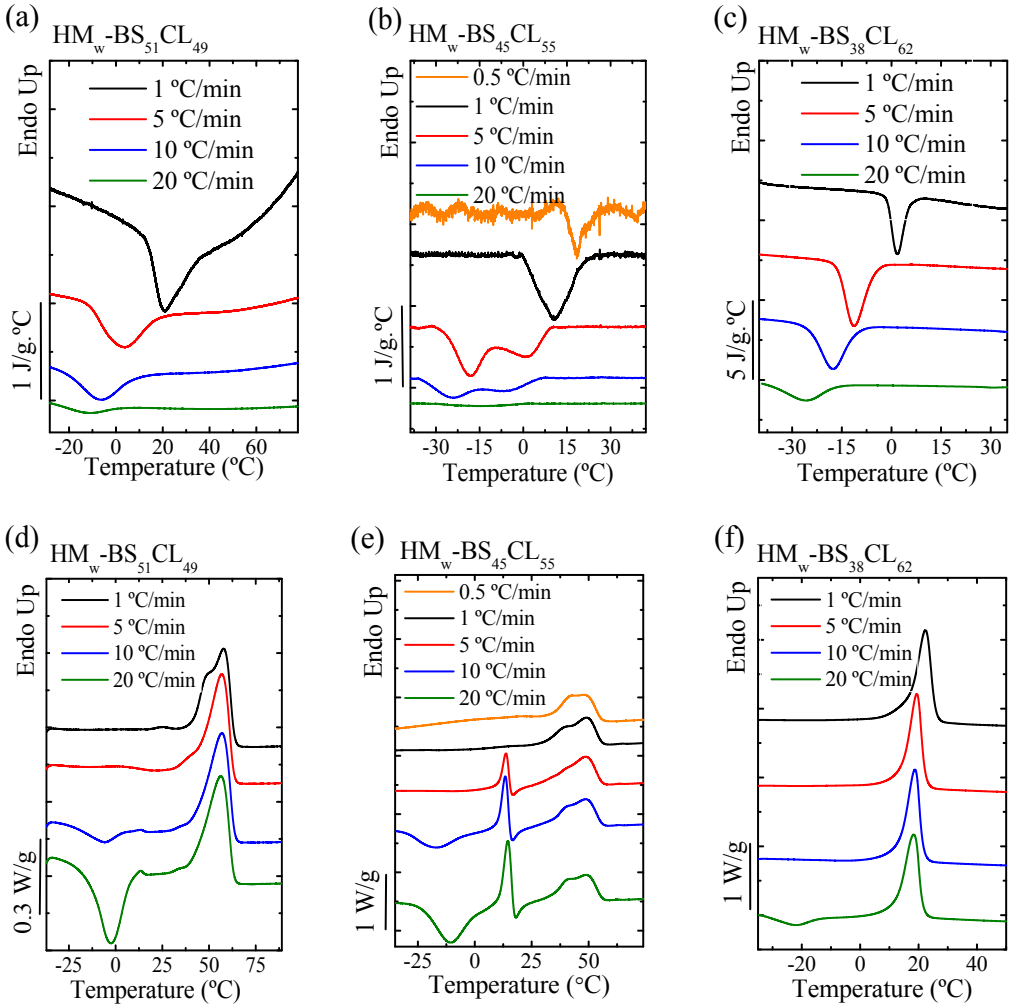

Figure 6. For HM_w copolyesters, $BS_{51}CL_{49}$ (a), $BS_{45}CL_{55}$(b), and $BS_{38}CL_{62}$(c) cooling scans to -60 °C at different cooling rates and (d), (e), (f) are subsequent heating scans performed at 20 °C/min for each copolyester.

At the pseudo-eutectic region, LM_w copolyesters exhibited some differences with HM_w samples. When the cooling rate was either slow or intermediate (1, 5 and 10 °C) both PBS and PCL-rich phases were able to crystallize, as indicated by the subsequent DSC scans (see Figures

SI-6 in the Supplementary Info). However, the amount of PCL-rich phase formed was still dependent on the cooling rate. As the cooling rate decreased, the amount of PBS-rich phase formed was much higher than that of PCL-rich phase. This increased ability of the PCL-rich phase to crystallize can be ascribed to the lower M_w of these copolyester samples which have demonstrated higher crystallization ability compatible with their increased X_c values in comparison to HM_w samples (Figure 3e).

The DSC cooling scans for HM_w samples in Figure 6b performed at 5 ºC/min shows a bimodal crystallization exotherm. When the subsequent heating DSC scan is examined in Figure 6e, the sample that was cooled at 5 ºC/min shows a clear but small melting peak at around 10 ºC, that corresponds to the melting of the PCL-rich phase. Notice the absence of cold crystallization before the PCL-rich crystals melt. At higher temperatures, a cold crystallization exotherm (which could be incomplete as a result of an overlap with the PCL-rich crystalline phase melting endotherm) of the PBS-rich phase can be observed, followed by the melting of the PBS-rich phase crystals. The DSC evidence clearly indicates that at 5 ºC/min, both PBS and PCL-rich phases are able to crystallize, but judging by their normalized melting enthalpies, the PBS-rich phase can crystallize much more (for PBS-rich phase ΔH_m=24 J/g and PCL-rich phase ΔH_m=5 J/g). A similar bimodal crystallization behavior occurred during cooling for compositions at the pseudo-eutectic region for LM_w copolyesters in Figure SI-6 b, c and d that were performed at 1 ºC/min and 5 ºC/min cooling rate.

Figure 7a shows PLOM micrographs taken during cooling from the melt at 5 º/min for the $BS_{45}CL_{55}$ HM_w copolymer sample, whose composition corresponds to the pseudo-eutectic point. At 0 ºC, a series of well-defined negative spherulites (with sizes close to 10 μm) with clear Maltese crosses can be seen, that correspond to the PBS-rich phase (as this is the first

component to crystallize, as corroborated by WAXS results presented below), surrounded by a melt of copolyester chains. Upon further cooling, at around -10 ºC, the PCL-rich phase starts to crystallize and additional small birefringent structures (circa 2 μm) were observed (together with small changes in the birefringence of the pre-existing spherulites, indicating that some PCL crystallization must have occurred inside the PBS-rich spherulitic templates, in analogy to Figure 2). Finally, at -30 ºC, two populations of spherulites coexist (although they are difficult to appreciate in Figure 7a, because of the scale of the micrograph), some are bigger (12 μm aprox) and are the double crystalline spherulites formed during cooling from the melt filled with both PBS-rich and PCL-rich lamellae. The second type are much smaller spherulites formed at temperatures of -10 ºC and lower, which must also correspond to double crystalline spherulites, although they may contain a higher population of PCL lamellae because they were formed at lower temperatures.

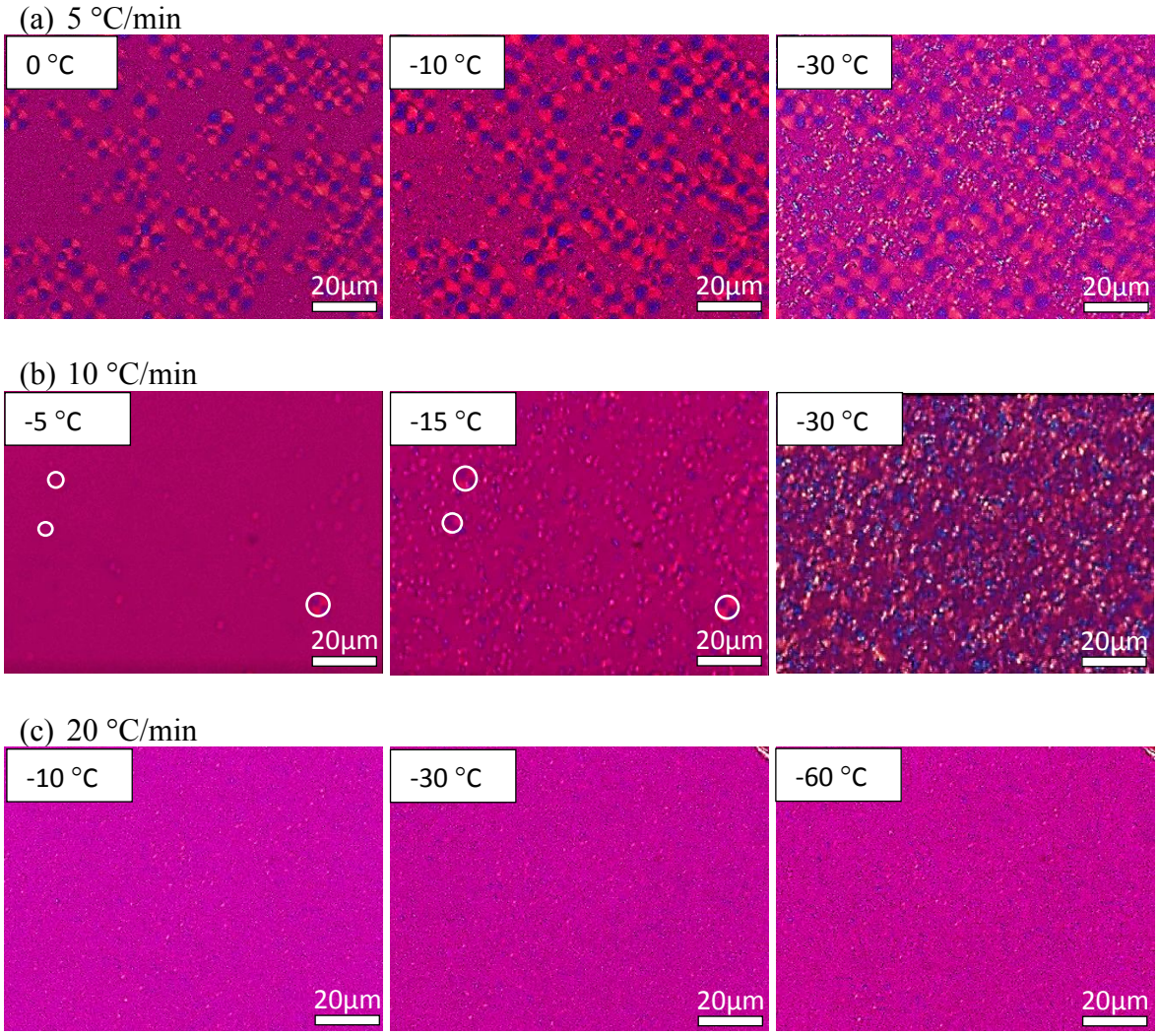

Figure 7. PLOM micrographs taken during cooling from the melt at different cooling rates for the HM_w $BS_{45}CL_{55}$ copolyester sample (whose composition corresponds to the pseudo-eutectic point): (a) 5 ºC/min, (b) 10 ºC/min, and (c) 20 ºC/min. The white scale bar is equal to 20 µm. The white circles in Figure 7b were drawn to highlight the presence of the few PBS-rich spherulites that were formed.

As the cooling rate increases to 10 ºC/min, the subsequent heating scans (performed always at 20 ºC/min) in Figure 6e show cold crystallization exotherms below the melting

transition of the PCL-rich phase melting. Figure 7b shows three PBS-rich phase spherulites (white circles were drawn to guide the eye) at higher temperature (-5 ºC) and at -15 ºC smaller birefringent structures appear that must correspond to PCL-rich phase spherulites. As WAXS experiments will demonstrate below, only PCL-rich crystals are detected at this cooling rate (10 ºC/min).

At an even higher cooling rate of 20 ºC/min, for both HM_w and LM_w copolyesters, the PBS-rich phase cannot crystallize at all during cooling, and only PCL-rich crystals are formed (see Figure 6b and 7c for the only HMw pseudo-eutectic composition copolymer; and Figures SI-6b, SI-6c, SI-6d for the 3 LMw pseudo-eutectic composition copolymers). The birefringent structures formed at 20 ºC/min, Figure 7c, corresponding to PCL-rich crystals are very small, with sizes barely discernible by PLOM.

In these interesting eutectic copolyester samples (HM_w $BS_{45}CL_{55}$ shown in Figures 6b and Figure 7 and LM_w $BS_{54}CL_{46}$, $BS_{48}CL_{52}$, $BS_{45}CL_{55}$ shown in the Supplementary Information), the control of the cooling rate is crucial, as the crystallinity and type of crystals formed strongly depend on this parameter.

Similar experiments were performed for two other copolymer samples, HM_w $BS_{51}CL_{49}$ whose composition fall to the left of the pseudo-eutectic point in Figure 1b, and HM_w $BS_{38}CL_{62}$, whose composition fall to the right of the pseudo-eutectic point. In both cases, only one phase was able to crystallize (i.e., the PBS-rich phase in HM_w $BS_{51}CL_{49}$ and the PCL-rich phase in HM_w $BS_{38}CL_{62}$) and the increase in cooling rate just caused a shift of the crystallization exotherm to lower temperatures as expected (together with a reduction in crystallization enthalpy), see Figures 6a and 6c. The subsequent heating scans are shown in Figures 6d and 6f

(performed at a constant heating rate of 20 ºC/min). The expected melting of the corresponding crystallizable phase (only one phase) can be observed, as well as cold crystallization in samples rapidly cooled. Parallel results were found for LM_w samples outside the pseudo-eutectic region and are shown in the Supplementary Information (see Figures SI-6a, 6e, 6f and 6j).

In summary, the crystallization of the PBS-rich and PCL-rich crystal phases have a strong dependence on cooling rate at the pseudo-eutectic point for both LM_w and HM_w copolymers. If the cooling rate is low enough (lower than 5 ºC/min), as the PBS-rich phase forms first during cooling from the melt, it produces spherulitic templates that had time to fully develop during slow cooling. The PCL-rich phase would have to crystallize within the PBS-rich interlamellar space and this does not happen in the HM_w copolymers, because of confinement effects.

When the cooling rate is intermediate (5 ºC/min), the PBS-rich phase can still form spherulitic templates (as indicated in Figure 7a), but they may not be as well structured as those formed at lower cooling rates, and the PCL-rich phase is able to develop some crystallinity. At a faster cooling rate of 10 ºC/min, only a few spherulites of the PBS-rich phase can form (marked by white circles in Figure 7b), and the PCL-phase crystallizes at lower temperatures and constitutes the majority of the crystal phase of the material.

At cooling rates of 20 ºC/min and faster, the PBS-rich phase cannot crystallize at all during cooling, giving the PCL-rich phase the possibility to develop some crystallinity during cooling (see Figure 7c). Upon subsequent heating, the PCL-rich phase can undergo cold-crystallization and enhances its crystallinity content. At even higher temperatures, the PBS-rich phase cold-crystallizes while the PCL-rich crystals melt.

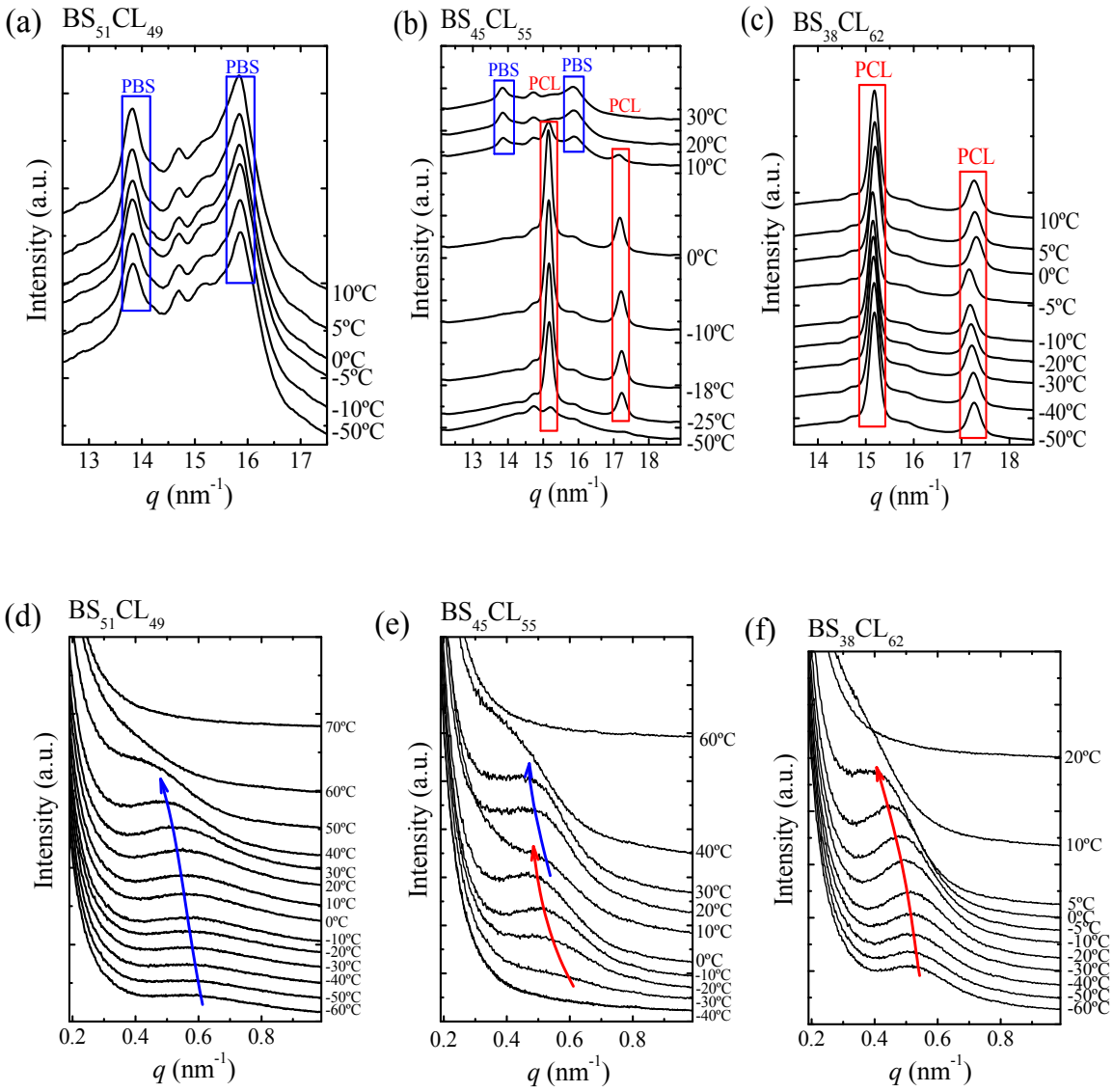

Figure 8. (a), (b), and (c) are WAXS patterns and (d), (e), and (f) are SAXS patterns during heating at 10 ºC/min (after cooling from the melt at 10 ºC/min) for the indicated copolyesters.

We performed *in situ* synchrotron SAXS/WAXS experiments for the 3 selected HM_w samples shown in Figure 6. These experiments were performed only at 10 ºC/min during both cooling and subsequent heating from the melt. The results obtained during heating at 10 ºC/min

(i.e., second heating, as the samples were first molten and then controlled cooled from the melt at 10 ºC/min) are presented in Figure 8, where selected diffractograms were chosen for a series of temperatures.

In the case of the two HM_w copolymer samples at each side of the pseudo-eutectic point, WAXS demonstrates that only one type of crystals is present, i.e., PBS like crystals for the $BS_{51}CL_{49}$ sample and PCL like crystals for the $BS_{38}CL_{62}$. These results are consistent with the previously discussed DSC data (Figure 6d and 6f, see the curves at 10 ºC/min). SAXS curves for these same copolymers also exhibit the expected behavior, as the SAXS maximum shifts to lower q values (higher long periods) as temperature is increased (see Figure 8), until the sample completely melts and a single phase isotropic melt is obtained.

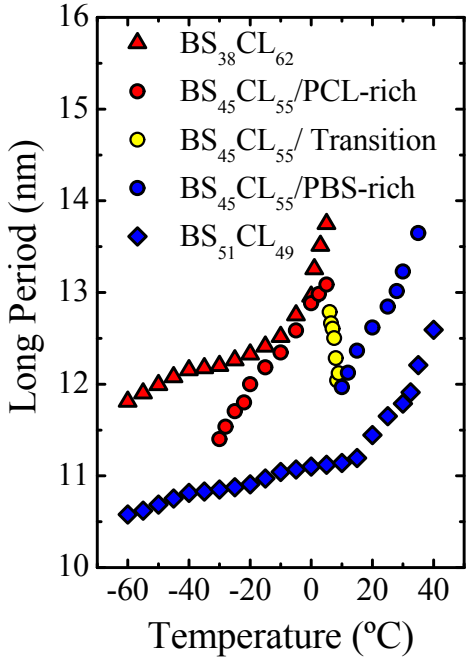

Figure 9. Long period values obtained from the SAXS maxima as a function of temperature during cooling for HM_w copolyester compositions close and at the pseudo-eutectic point.

The most interesting results are those obtained for the copolymer composition at the pseudo-eutectic point, i.e., the HM_w $BS_{45}CL_{55}$ copolyester sample. Figure 8b should be read from bottom to top, as the sample was being heated, and it should be compared with Figure 6e (i.e., specifically with the DSC heating trace performed at 10 ºC/min).

Firstly, it is interesting to note that according to WAXS data, the PCL-rich phase is the only one whose crystallization can be detected during cooling at 10 ºC/min (see WAXS patterns taken during cooling at 10 ºC/min in Figure SI-7a), since the low temperature WAXS traces only show reflections that correspond to PCL (see the selected temperatures of -50, -25, -18, -10 and 0 ºC in Figure 8b). The DSC cooling curve, on the other hand, in Figure 6b shows a bimodal exotherm, that we interpret as arising from the crystallization of the PBS-rich component first (at higher temperatures) and then of the PCL component, at lower temperatures. However, the WAXS data shows that if such crystallization from the PBS phase occurs, it cannot be detected by WAXS. This is probably due to the lateral size of the crystals, which are too small for WAXS detection. However, PLOM results shown in Figure 7b, also evidenced the presence of a very small population of spherulites at -5 ºC, suggesting that a small amount of PBS-rich crystals are indeed formed during cooling from the melt, in accordance with the DSC data presented in Figure 6b.

The DSC heating scan in Figure 6e does show the melting of both phases during heating, but there is a strong cold crystallization exotherm located in the range -10 to 0 ºC, where WAXS evidences the crystallization of the PCL-rich crystalline phase (Figure 8b). In fact, at temperatures of -50 ºC, the WAXS trace in Figure 8b indicates a very low degree of crystallinity for the PCL-rich phase (as judged by the area under the crystalline reflections). Such degree of

crystallinity increases upon heating in a consistent way as the PCL-rich phase undergoes cold crystallization.

The PBS-rich phase only starts to crystallize during heating at 10 ºC, a temperature at which, according to DSC data (Figure 6e), PCL is in the process of melting. WAXS also shows a strong decrease in the PCL (110) reflection at 10 ºC (Figure 8b). Therefore, a comparison between DSC and WAXS indicates that there is an overlap between the melting of the PCL-rich phase and the cold crystallization of the PBS-rich phase.

Figure 8e shows the SAXS patterns as a function of temperature during heating of the $BS_{45}CL_{55}$ sample at 10 ºC/min. Even though a single SAXS peak can be observed for all temperatures, the trend in peak position and widths of the curves changes with temperature. The biggest change occurs above 0 ºC, when the PCL-rich crystals start to melt and new PBS-rich crystals are formed by a cold-crystallization process.

Figure 9 plots the long periods obtained from the SAXS maxima as a function of temperature for the three samples examined. The increase in long periods with temperature is a common trend observed in semi-crystalline materials, as lamellar crystals tend to reorganize by thickening during heating (at temperatures below their melting points). At temperatures where partial melting occurs, the long period increases, typically more rapidly, as the average distance between lamellae increases as the fraction of molten polymer increases.

The sample whose composition is at the pseudo-eutectic point shows in Figure 9 a clear transition region, where the long period briefly decreases with temperature, exactly at the temperature region where PCL-rich crystals melt and PBS-rich crystals form. At temperatures below the transition, the long period is dominated by the PCL-rich lamellar crystals and above

the transition by the PBS-rich lamellar crystals, as the comparison with the other two copolyester samples clearly suggests. The results are consistent with WAXS, DSC and PLOM results.

Conclusions

The HM_w synthesized copolymers are also isodimorphic, as our previously prepared analogous LM_w copolyesters. Nevertheless, the effect of molecular weight is very interesting. We found that T_c and T_m values, as well as lamellar thickness values, are insensitive to large molecular weight variations as they are determined by the average lengths of the crystallizable sequences which in turn are a function of the randomness of the comonomer sequence distribution and hence their selection during crystallization. However, both the crystallinity degree (as well as the long period values which depend on it) and the T_g of the copolymers did vary significantly with increases in molecular weight, as their values depend on the entire chain length and chain mobility. Therefore, changing the molecular weight of the copolymer affords separate control over T_g and T_m depending on composition.

The copolymers display spherulitic superstructures whose nucleation depends on copolymer composition. At the pseudo-eutectic point, HM_w $BS_{45}CL_{55}$ copolyester was the only double crystalline copolymer, whose PBS-rich phase forms space filling spherulites at higher temperatures that template the superstructural morphology of the copolymer. These PBS-rich phase spherulites contain radial lamellar stacks. After cooling down to lower temperatures, the PCL-rich phase crystallizes in the interlamellar (intraspherulitic) amorphous regions with newly formed lamellae.

Comonomer exclusion limits the average length of the crystallizable sequences and therefore l_c decreases when comonomer addition increases at each side of the pseudo-eutectic region. Comonomer exclusion also limits the amount of crystals that can be formed and the degree of crystallinity also decreases with comonomer content while l_a increases at each side of the pseudo-eutectic region.

In the specific cases of the HM_w $BS_{45}CL_{55}$, LM_w $BS_{54}CL_{46,}$ LM_w $BS_{48}CL_{52}$ and LM_w $BS_{45}CL_{55}$ copolyesters (whose compositions correspond to the pseudo-eutectic point or region), our results indicate that the cooling rate can determine which phase can crystallize and also if a single phase or two phases are formed. Very low cooling rates (below 5 ºC/min) lead to the formation of only PBS-rich crystals in HM_w, although for LM_w both PBS-rich and PCL-rich phases can crystallize. Intermediate cooling rates allow the formation of double crystalline spherulites composed by PBS-rich and PCL-rich lamellae in both HM_w and LM_w copolyesters. Finally, for both HM_w and LM_w copolyesters when heating rates are as high as 20 ºC/min, only PCL-rich crystals can form. In this way, the morphology and thermal transitions of this copolyester at the pseudo-eutectic composition can be tailored for specific applications.

Acknowledgments

M.S. gratefully acknowledges the award of a PhD fellowship by POLYMAT Basque Center for Macromolecular Design and Engineering. The POLYMAT/UPV/EHU and UPC teams would like to acknowledge funding from MINECO through projects MAT2017-83014-C2-1-P and MAT-2016-77345-CO3-02 respectively, and from ALBA synchrotron facility through granted proposal 2017082318 (March 2018).

Supporting Information

Complementary NMR characterization data (Figures SI-1 and SI-2), DSC Data (Figures SI-3 and SI-4), Polarized light Optical Micrographs (Figure SI-5) and effect of cooling rates on thermal properties (Figure SI-6) and WAXS (Figure SI-7), and WAXS data as a function of copolymer composition (SI-8). Tables SI-1–SI-5 report GPC, NMR, calorimetric and X-ray diffraction data.

References

1. Pérez-Camargo, R. A.; Arandia, I.; Safari, M.; Cavallo, D.; Lotti, N.; Soccio, M.; Müller, A. J. Crystallization of isodimorphic aliphatic random copolyesters: Pseudo-eutectic behavior and double-crystalline materials. *European Polymer Journal* **2018,** 101, 233-247, DOI: 10.1016/j.eurpolymj.2018.02.037.

2. Natta, G.; Corradini, P.; Sianesi, D.; Morero, D. Isomorphism phenomena in macromolecules. *Journal of Polymer Science* **1961,** 51 (156), 527-539, DOI: 10.1002/pol.1961.1205115610

3. Allegra, G.; Bassi, I., Isomorphism in synthetic macromolecular systems. In *Fortschritte der Hochpolymeren-Forschung*, Springer: Berlin, 1969; pp 549-574.

4. Yu, Y.; Sang, L.; Wei, Z.; Leng, X.; Li, Y. Unique isodimorphism and isomorphism behaviors of even-odd poly (hexamethylene dicarboxylate) aliphatic copolyesters. *Polymer* **2017,** 115, 106-117, DOI: 10.1016/j.polymer.2017.03.034.

5. Latere Dwan'Isa, J.-P.; Lecomte, P.; Dubois, P.; Jérôme, R. Synthesis and characterization of random copolyesters of ε-caprolactone and 2-oxepane-1, 5-dione. *Macromolecules* **2003,** 36 (8), 2609-2615, DOI: 10.1021/ma025973t.

6. Ye, H.-M.; Wang, R.-D.; Liu, J.; Xu, J.; Guo, B.-H. Isomorphism in poly (butylene succinate-co-butylene fumarate) and its application as polymeric nucleating agent for poly (butylene succinate). *Macromolecules* **2012,** 45 (14), 5667-5675, DOI: 10.1021/ma300685f.

7. Ceccorulli, G.; Scandola, M.; Kumar, A.; Kalra, B.; Gross, R. A. Cocrystallization of random copolymers of ω-pentadecalactone and ε-caprolactone synthesized by lipase catalysis. *Biomacromolecules* **2005,** 6 (2), 902-907, DOI: 10.1021/bm0493279.

8. Yu, Y.; Wei, Z.; Liu, Y.; Hua, Z.; Leng, X.; Li, Y. Effect of chain length of comonomeric diols on competition and miscibility of isodimorphism: A comparative study of poly (butylene glutarate-co-butylene azelate) and poly (octylene glutarate-co-octylene azelate). *European Polymer Journal* **2018,** 105, 274-285, DOI: 10.1016/j.eurpolymj.2018.06.006.

9. Siracusa, V.; Gazzano, M.; Finelli, L.; Lotti, N.; Munari, A. Cocrystallization phenomena in novel poly (diethylene terephthalate-co-thiodiethylene terephthalate) copolyesters. *Journal of Polymer Science Part B: Polymer Physics* **2006,** 44 (11), 1562-1571, DOI: 10.1002/polb.20819

10. Morales-Huerta, J. C.; Martinez de Ilarduya, A.; Muñoz-Guerra, S. n. Sustainable aromatic copolyesters via ring opening polymerization: poly (butylene 2, 5-furandicarboxylate-co-terephthalate) s. *ACS Sustainable Chemistry & Engineering* **2016,** 4 (9), 4965-4973, DOI: 10.1021/acssuschemeng.6b01302.

11. Li, X.; Hong, Z.; Sun, J.; Geng, Y.; Huang, Y.; An, H.; Ma, Z.; Zhao, B.; Shao, C.; Fang, Y. Identifying the phase behavior of biodegradable poly (hexamethylene succinate-co-hexamethylene adipate) copolymers with FTIR. *The Journal of Physical Chemistry B* **2009,** 113 (9), 2695-2704, DOI: 10.1021/jp8061866.

12. Hong, M.; Tang, X.; Newell, B. S.; Chen, E. Y.-X. "Nonstrained" γ-Butyrolactone-Based Copolyesters: Copolymerization Characteristics and Composition-Dependent (Thermal, Eutectic, Cocrystallization, and Degradation) Properties. *Macromolecules* **2017,** 50 (21), 8469-8479, DOI: 10.1021/acs.macromol.7b02174.

13. Yu, Y.; Wei, Z.; Zhou, C.; Zheng, L.; Leng, X.; Li, Y. Miscibility and competition of cocrystallization behavior of poly (hexamethylene dicarboxylate) s aliphatic copolyesters: effect of chain length of aliphatic diacids. *European Polymer Journal* **2017,** 92, 71-85, DOI: 10.1016/j.eurpolymj.2017.04.036.

14. Liang, Z.; Pan, P.; Zhu, B.; Dong, T.; Hua, L.; Inoue, Y. Crystalline phase of isomorphic poly (hexamethylene sebacate-co-hexamethylene adipate) copolyester: Effects of comonomer composition and crystallization temperature. *Macromolecules* **2010,** 43 (6), 2925-2932, DOI: 10.1021/ma1000546.

15. Papageorgiou, G. Z.; Bikiaris, D. N. Synthesis and Properties of Novel Biodegradable/Biocompatible Poly [propylene-co-(ethylene succinate)] Random Copolyesters. *Macromolecular Chemistry and Physics* **2009,** 210 (17), 1408-1421, DOI: 10.1002/macp.200900132.

16. Pérez-Camargo, R. A.; Fernández-d'Arlas, B.; Cavallo, D.; Debuissy, T.; Pollet, E.; Avérous, L.; Müller, A. J. Tailoring the structure, morphology, and crystallization of isodimorphic poly (butylene succinate-ran-butylene adipate) random copolymers by changing composition and thermal history. *Macromolecules* **2017,** 50 (2), 597-608, DOI: 10.1021/acs.macromol.6b02457.

17. Debuissy, T.; Sangwan, P.; Pollet, E.; Avérous, L. Study on the structure-properties relationship of biodegradable and biobased aliphatic copolyesters based on 1, 3-propanediol, 1, 4-butanediol, succinic and adipic acids. *Polymer* **2017,** 122, 105-116, DOI: 10.1016/j.polymer.2017.06.045.

18. Wang, K.; Jia, Y.-G.; Zhu, X. Two-Way Reversible Shape Memory Polymers Made of Cross-Linked Cocrystallizable Random Copolymers with Tunable Actuation Temperatures. *Macromolecules* **2017,** 50 (21), 8570-8579, DOI: 10.1021/acs.macromol.7b01815.

19. Soccio, M.; Finelli, L.; Lotti, N.; Gazzano, M.; Munari, A. Poly (propylene isophthalate), poly (propylene succinate), and their random copolymers: synthesis and thermal properties. *Journal of Polymer Science Part B: Polymer Physics* **2007,** 45 (3), 310-321, DOI: 10.1002/polb.21049

20. Soccio, M.; Finelli, L.; Lotti, N.; Gazzano, M.; Munari, A. Novel random poly (propylene isophthalate/adipate) copolyesters: Synthesis and characterization. *European polymer journal* **2006,** 42 (11), 2949-2958, DOI: 10.1016/j.eurpolymj.2006.07.016.

21. Lendlein, A.; Sisson, A., *Handbook of biodegradable polymers: isolation, synthesis, characterization and applications*. John Wiley & Sons: Weinheim, 2011.

22. Bechthold, I.; Bretz, K.; Kabasci, S.; Kopitzky, R.; Springer, A. Succinic acid: a new platform chemical for biobased polymers from renewable resources. *Chemical Engineering & Technology* **2008,** 31 (5), 647-654, DOI: 10.1002/ceat.200800063.

23. Zheng, L.; Li, C.; Wang, Z.; Wang, J.; Xiao, Y.; Zhang, D.; Guan, G. Novel biodegradable and double crystalline multiblock copolymers comprising of poly (butylene succinate) and poly (ε-caprolactone): synthesis, characterization, and properties. *Industrial & Engineering Chemistry Research* **2012,** 51 (21), 7264-7272, DOI: 10.1021/ie300576z.

24. Qiu, Z.; Komura, M.; Ikehara, T.; Nishi, T. Miscibility and crystallization behavior of biodegradable blends of two aliphatic polyesters. Poly (butylene succinate) and poly (ε-caprolactone). *Polymer* **2003,** 44 (25), 7749-7756, DOI: 10.1016/j.polymer.2003.10.013.

25. Alamo, R. G.; Viers, B. D.; Mandelkern, L. Phase structure of random ethylene copolymers: a study of counit content and molecular weight as independent variables. *Macromolecules* **1993,** 26 (21), 5740-5747, DOI: 10.1021/ma00073a031.

26. Di Lorenzo, M.; Silvestre, C. Non-isothermal crystallization of polymers. *Progress in Polymer Science* **1999,** 24 (6), 917-950, DOI: 10.1016/S0079-6700(99)00019-2.

27. Ciulik, C.; Safari, M.; Martínez de Ilarduya, A.; Morales-Huerta, J. C.; Iturrospe, A.; Arbe, A.; Müller, A. J.; Muñoz-Guerra, S. Poly (butylene succinate-ran-ε-caprolactone) copolyesters: Enzymatic synthesis and crystalline isodimorphic character. *European Polymer Journal* **2017,** 95, 795-808, DOI: 10.1016/j.eurpolymj.2017.05.002.

28. Cao, A.; Okamura, T.; Ishiguro, C.; Nakayama, K.; Inoue, Y.; Masuda, T. Studies on syntheses and physical characterization of biodegradable aliphatic poly (butylene succinate-co-ε-caprolactone) s. *Polymer* **2002,** 43 (3), 671-679, 10.1016/S0032-3861(01)00658-9.

29. Arandia, I.; Mugica, A.; Zubitur, M.; Arbe, A.; Liu, G.; Wang, D.; Mincheva, R.; Dubois, P.; Müller, A. J. How composition determines the properties of isodimorphic poly (butylene succinate-ran-butylene azelate) random biobased copolymers: from single to double crystalline random copolymers. *Macromolecules* **2014,** 48 (1), 43-57, DOI: 10.1021/ma5023567.

30. Castillo, R.; Müller, A. Crystallization and morphology of biodegradable or biostable single and double crystalline block copolymers. *Progress in Polymer Science* **2009,** 34 (6), 516-560, DOI: 10.1016/j.progpolymsci.2009.03.002.

31. Palacios, J. K.; Mugica, A.; Zubitur, M.; Müller, A. J., Crystallization and Morphology of Block Copolymers and Terpolymers With More Than One Crystallizable Block. In *Crystallization in Multiphase Polymer Systems*, Elsevier: **2018**; pp 123-180, DOI: 10.1016/B978-0-12-809453-2.00006-2.

32. Mandelkern, L., *Crystallization of polymers*. 2nd edition ed.; Cambridge University Press: Cambridge 2002; Vol. 1, Equilibrium Concepts, DOI: 10.1017/CBO9780511535413.001.

33. Van Krevelen, D. W.; Te Nijenhuis, K., *Properties of polymers: their correlation with chemical structure; their numerical estimation and prediction from additive group contributions*. Elsevier: Amsterdam, 2009.

34. Pitt, C. G.; Chasalow, F.; Hibionada, Y.; Klimas, D.; Schindler, A. Aliphatic polyesters. I. The degradation of poly (ϵ-caprolactone) in vivo. *Journal of Applied Polymer Science* **1981,** 26 (11), 3779-3787, DOI: 10.1002/app.1981.070261124.

35. Hiemenz, P. C.; Lodge, T. P., *Polymer chemistry*. CRC press: Boca Raton, 2007.

36. Schneider, H.; Rieger, J.; Penzel, E. The glass transition temperature of random copolymers: 2. Extension of the Gordon-Taylor equation for asymmetric Tg vs composition curves. *Polymer* **1997,** 38 (6), 1323-1337, DOI: 10.1016/S0032-3861(96)00652-0.

37. Simha, R.; Boyer, R. On a general relation involving the glass temperature and coefficients of expansion of polymers. *The Journal of Chemical Physics* **1962,** 37 (5), 1003-1007, DOI: 10.1063/1.1733201.

38. Pinal, R. Entropy of mixing and the glass transition of amorphous mixtures. *Entropy* **2008,** 10 (3), 207-223, DOI:10.3390/entropy-e10030207.

39. Penzel, E.; Rieger, J.; Schneider, H. The glass transition temperature of random copolymers: 1. Experimental data and the Gordon-Taylor equation. *Polymer* **1997,** 38 (2), 325-337, DOI: 10.1016/S0032-3861(96)00521-6.

40. Díaz, A.; Franco, L.; Puiggalí, J. Study on the crystallization of poly (butylene azelate-co-butylene succinate) copolymers. *Thermochimica Acta* **2014,** 575, 45-54, DOI: 10.1016/j.tca.2013.10.013.

For table of contents use only

Tuning the thermal properties and morphology of isodimorphic poly[(butylene succinate)-*ran*-(ε-caprolactone)] copolyesters by changing composition, molecular weight and thermal history

Maryam Safari[1], Antxon Martínez de Ilarduya[2], Agurtzane Mugica[1], Manuela Zubitur[3], Sebastián Muñoz-Guerra[2], Alejandro J. Müller*[1,4]